



Comparing the performance of four shading strategies based on a multi-objective genetic algorithm: A case study in a university library

Shikang Wen ^a, Xiao Hu ^a, Guanjun Hua ^a, Peng Xue ^b, Dayi Lai ^{a,*}

^a Department of Architecture, School of Design, Shanghai Jiao Tong University, Shanghai, 200240, China

^b Beijing Key Laboratory of Green Built Environment and Energy Efficient Technology, Beijing University of Technology, Beijing, 100124, China



ARTICLE INFO

Keywords:

Multi-objective genetic algorithm
Shading strategy optimization
Daylight environment
Glare
Visual comfort
Pareto set
Artificial neural network

ABSTRACT

Through the control of excessive daylight in buildings, shading devices can reduce glare and improve occupants' visual comfort. However, shading devices may overly reduce illuminance levels. Many shading strategies are available, but they do not perform equally well, and traditionally, it has been difficult to select the most suitable shading strategy. This study proposed a parameterization method for the selection and design of a shading strategy that would reduce glare while maintaining a satisfactory daylighting level, through the construction of Pareto sets based on a multi-objective genetic algorithm. The objective function was created by combining a dynamic glare evaluation indicator, the spatial glare autonomy (sGA), and a self-constructed daylight index, the spatial daylight vote autonomy (sDVA), developed from a field survey. As a case study, the proposed method was used to compare the performance of four shading strategies, including vertical slats (Vs), a perforated aluminum sheet (PAS), serrated windows with southern orientation (Sw_S), and serrated windows with northern orientation (Sw_N) in a university library in Shanghai, China. It was found that the Sw_S and PAS had a relatively bad performance; the Vs performed better than the Sw_N in providing a more satisfactory illuminance level; and the Sw_N was more effective in reducing the glare. The multi-objective optimization process can be used to obtain near-optimal design parameters that create a visual environment with reduced glare while maintaining an acceptable illuminance level, for all four shading strategies. The developed method can be a helpful tool in the design of an appropriate daylighting environment.

* Corresponding author.

E-mail address: dayi_lai@sjtu.edu.cn (D. Lai).

Nomenclature

Abbreviations

ANN	Artificial Neural Network
ASE	Annual Sunlight Exposure
CFS	Complex Fenestration Systems
CI	Confidence Interval
DGP	Daylight Glare Probability
DGI	Daylight Glare Index
DA	Daylight Autonomy
DVA	Daylight Vote Autonomy
Hs	Horizontal slats
MOGA	Multi-Objective Genetic Algorithm
MSE	Mean Square Error
MAE	Mean Absolute Error
NSGA-II	Nondominated Sorting Genetic Algorithm-II
PAS	Perforated Aluminum Sheet
PSO	Particle Swarm Optimization
RMSE	Root Mean Square Error
R ²	The coefficient of determination
Sw	Serrated windows
Sw_S	Serrated windows facing South
Sw_N	Serrated windows facing North
SOGA	Single-Objective Genetic Algorithm
sDA	Spatial Daylight Autonomy
sDVA	Spatial Daylight Vote Autonomy
sDVAbest	Best performance of sDVA
sDVA0.30/80%	The sDVA that DSV threshold to 0.30 and temporal fraction threshold to 80%
sGA	Spatial Glare Autonomy
sGAbest	Best performance of sGA
sGA0.35/95%	The sGA that DGP threshold to 0.35 and temporal fraction threshold to 95%
TCI	Thermal Comfort Index
TEC	Total Energy Consumption
UDI	Useful Daylight Illuminance
Vs	Vertical Slats
WWR	Window-to-Wall Ratio

Symbols

dt_i	The amount of time lower than the daylight subjective vote (DSV) threshold of sDVA at point i
E_h	Horizontal illuminance (lux)
gt_i	The quantity lower than the Daylight Glare Probability (DGP) threshold of sGA at point i
lux	Illuminance (lm/m^2)
L_s	The luminance of the glare source (lux)
n	The number of glare sources
P	The position index
t_x	The number of annual daytime hours
t_y	The number of annual daytime hours
ω_s	The solid angle of the glare source
τ	The temporal fraction threshold
γ	The temporal fraction threshold

1. Introduction

Lighting accounts for 15% of the total energy consumption (TEC) in buildings [1]. Daylighting, as a passive strategy, is an important way to reduce energy consumption and carbon emission. At the same time, natural light has health benefits [2,3] and can improve occupants' working efficiency [4,5]. According to Xue et al. [6], occupants' luminous comfort is most influenced by their level of satisfaction with natural light. However, uncontrolled excessive daylight will cause glaring problems [7]. For example, Beck et al. [8] found that excessive direct sunlight in some school buildings resulted in increased levels of visual discomfort due to glare.

Table 1

Strategies, objective functions, and optimization algorithms were used in previous studies.

Author and Year of Publication	Shading strategy				Objective function							Optimization algorithm			
	Hs	Vs	CFS	WWR	DGP	DGI	sDA	ASE	UDI	TCI	Illuminance	TEC	SOGA	MOGA	PSO
Torres and Sakamoto 2007 [10]		✓			✓						✓		✓		
Gagne and Andersen 2010 [15]	✓	✓		✓	✓						✓			✓	
Lartigue et al., 2013 [13]				✓							✓		✓	✓	
Manzan 2014 [11]	✓									✓			✓	✓	
González and Fiorito 2015 [16]	✓								✓		✓		✓	✓	
Vera et al., 2017 [12]			✓					✓	✓			✓			✓
Kirimtat et al., 2019 [17]	✓								✓			✓		✓	
Zhai et al., 2019 [18]				✓						✓	✓		✓	✓	
Jalali et al., 2020 [19]				✓					✓				✓	✓	
Bakmohammadi and Noorzai 2020 [20]			✓	✓	✓				✓(DA)		✓		✓	✓	
Naderi et al., 2020 [21]	✓					✓					✓		✓	✓	
Pilechiha, Mahdavinejad et al., 2020 [22]				✓			✓	✓					✓	✓	
Bahdad et al., 2021 [23]	✓				✓				✓				✓	✓	
Ishac and Nadim 2021 [24]	✓				✓						✓			✓	
Khidmat, Fukuda et al., 2022 [25]				✓		✓		✓						✓	

Shading strategies: Hs = Horizontal slats; Vs = Vertical slats; CFS = Complex Fenestration Systems; WWR = Window-to-Wall Ratio; Sw = Serrated windows;

Objective functions: DGP = Daylight Glare Probability; DGI = Daylight Glare Index; sDA = spatial Daylight Autonomy; ASE = Annual Sunlight Exposure; UDI = Useful Daylight Illuminance; TCI = Thermal Comfort Index; TEC = Total Energy Consumption;

Optimization algorithm: SOGA = Single-Objective Genetic Algorithm; MOGA = Multi-Objective Genetic Algorithm; PSO = Particle Swarm Optimization.

Therefore, shading systems are used to control direct daylight and prevent visual discomfort [9].

Although shading systems can block direct sunlight and reduce glare, the addition of shading devices may overly reduce horizontal illuminance levels, which in turn decreases occupants' satisfaction with the daylight environment. Changing the design may improve one performance metric but worsen another. Thus, the design of a shading system is a multi-objective problem with contradictory goals. Many researchers have conducted optimization studies on shading strategies with various objectives, as summarized in Table 1. For instance, Torres and Sakamoto [10] optimized the size, number, and position of vertical slats (Vs) by combining the daylight glare probability (DGP) and illuminance as the objective function. Manzan [11] studied the design of horizontal slats (Hs) and obtained a design solution that reduced energy consumption by 19% in Trieste and 30% in Rome. Vera et al. [12] optimized a complex fenestration system (CFS) with spatial daylight autonomy (sDA), annual sunlight exposure (ASE), and TEC as design objectives. Other researchers [13,14] optimized the window-to-wall ratio (WWR) based on daylight performance and air conditioning load. These studies have provided useful frameworks and valuable information for finding an appropriate design parameter for shading components.

However, the above studies each focused on only a single strategy. In practice, different shading systems have different

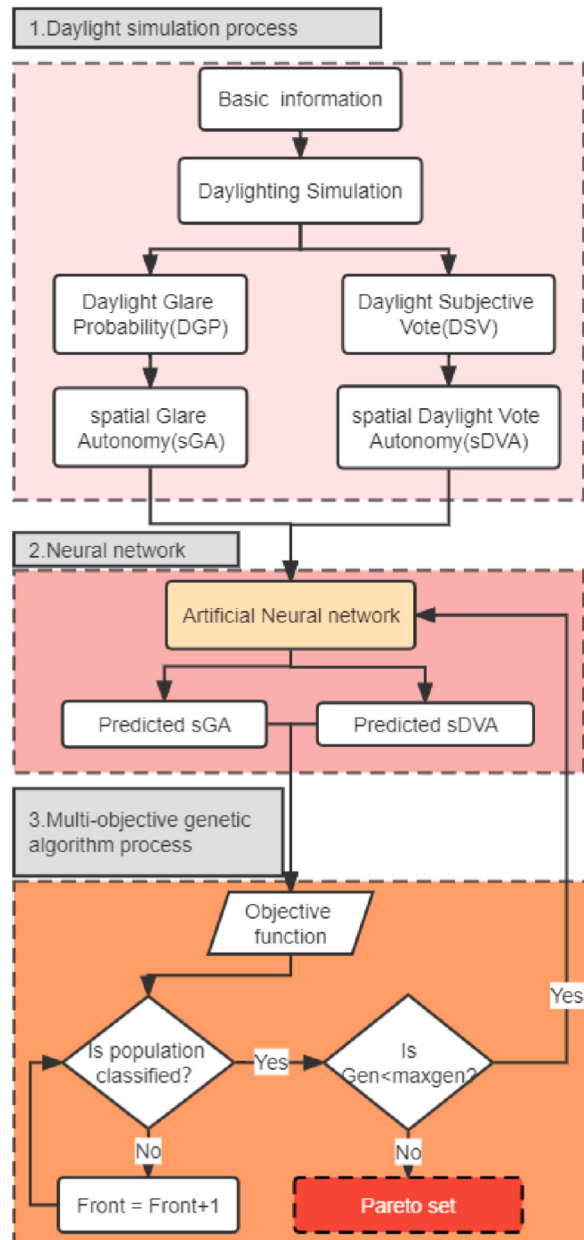


Fig. 1. The process used to optimize a shading device based on MOGA.

“performance curves”. When designing a suitable daylight environment, it is essential to compare the performance of various shading strategies. Wienold et al. [26] simulated and compared the energy and comfort performance of different shading strategies including venetian blind, Retrolux blind, and venetian blind + rollo blind. Day et al. [27] evaluated three shading strategies, including automated Venetian slats, electrochromic glass, and automated fabric shade screens, by subjective perception. The strategies in Refs. [26, 27] were only compared at fixed constructions, whereas the performance of a shading system varies with the design parameters. Thus, a comprehensive comparison with ranges of design parameters is necessary.

This study proposed a standard method for comparing the performance of different shading strategies. The method was applied in a university library as a case study, and four shading strategies, serrated windows with southern orientation, serrated windows with northern orientation, vertical slats, and a perforated aluminum sheet, were selected and compared in terms of their ability to reduce glare and maintain a satisfactory illuminance level. The following sections describe our method and findings.

2. Methods

This section introduces the overall process, simulation tools, artificial neural networks, and objective function for the shading strategy optimization and comparison. We validated the daylighting simulation engine by comparing the predicted illuminance with the measurement results. We then conducted field surveys to develop a formula to calculate the daylight subjective vote (DSV), which is an important component of the objective function. Finally, four shading strategies, namely, a perforated aluminum sheet (PAS), vertical slats (Vs), serrated windows with southern orientation (Sw_S), and serrated windows with northern orientation (Sw_N), were selected for further comparison in a university library as a case study.

2.1. Process

This study attempted to optimize the design parameters of a shading device to reduce glare and improve occupants' visual satisfaction with the daylit space. As displayed in Fig. 1, the optimization process consists of three parts: daylight simulation, artificial neural network (ANN) modeling, and a multi-objective genetic algorithm (MOGA) process. The daylight simulation aims to obtain an objective function, while the MOGA optimizes the design parameters of the shading device based on the objective function. In addition, we use ANN to reduce the simulation time. The following subsections describe the daylight simulation process, the setting of the objective function, ANN modeling, and the MOGA process.

2.1.1. Daylight simulation

First, daylight simulation is conducted to obtain the value of the objective function, which serves as the basis for optimization. The Ladybug and Honeybee platforms from the Grasshopper plugin in Rhino were used for the simulation. The daylight simulation engine was based on Radiance software [28]. The geometry of the tested building and shading device needs to be created with material properties. Weather information is used to drive the simulation for a certain period. The daylight glare probability (DGP) at test viewpoints and the illuminance at test points are then obtained for the calculated location of the objective function. The simulated period is set to daylight hours throughout the year to better evaluate the effect of the shading device dynamically.

2.1.2. Objective function

To minimize glare and maximize occupants' visual satisfaction in a dynamic daylight environment, the objective function is set as:

$$\left\{ \begin{array}{l} \min(sGA) \\ \min(sDVA) \end{array} \right. \quad (1)$$

where sGA is the spatial glare autonomy, and sDVA is spatial daylight vote autonomy. sGA was established by Jones [29], and it is about the percentage of test points that meet the defined minimum fraction of glare-free during daylight hours of a year. The sGA equation is as follows:

$$sGA = \frac{\sum_{i=1}^N GT(i)}{N}, \text{ with } GT(i) = \begin{cases} 1 & : gt_i \geq \tau t_x \\ 0 & : gt_i < \tau t_x \end{cases} \quad (2)$$

where gt_i is the quantity lower than the DGP threshold of sGA at point i, t_x represents the number of annual daytime hours, τ the temporal fraction threshold. In this study, we set the DGP threshold to 0.35 and τ to 95%, namely, sGA0.35/95%. Some researchers [30–32] has reported that dynamic metrics is more appreciated for assessing the annual dynamic daylit space than static metric. The sGA was the dynamic metric for assessing the glare discomfort of daylit space and was developed according to daylight glare probability (DGP). Therefore, the DGP threshold is important for the calculation of sGA. Table 3 shows the correlation between DGP and glare level. In addition, the DGP can be represented as the equation:

$$DGP = 5.87 \times 10^{-5} E_v + 9.18 \times 10^{-2} \log \left(\sum_i^n \frac{L_{s,i}^2 \omega_{s,i}}{E_v^{1.87} P_i^2} \right) + 0.16 \quad (3)$$

where E_v the vertical illuminance (lux), L_s the luminance of the glare source (lux), ω_s the solid angle of the glare source, P the position index, and n the number of glare sources.

In objective function (1), sDVA is used to quantify people's satisfaction with the dynamic daylight environment. It is reported as the ratio of test points that received a specific minimum fraction of satisfactory threshold during the daylight hours of a year. The sDVA

equation is represented as:

$$sDVA = \frac{\sum_{i=1}^N DT(i)}{N}, \text{ with } DT(i) = \begin{cases} 1 & : dt_i \geq \gamma t_y \\ 0 & : dt_i < \gamma t_y \end{cases} \quad (4)$$

where dt_i is the amount of time lower than the daylight subjective vote (DSV) threshold of sDVA at point i, t_y represents the number of annual daytime hours, γ the temporal fraction threshold. For maintaining the satisfaction level, the temporal fraction of the DSV threshold would refer to the daylight performance of the study case. In this study, we set the DSV threshold to 0.30 and γ to 80% which equates to the average daylight vote autonomy (DVA) in the original daylight environment of the study case, namely, sDVA0.30/80%. The satisfaction with daylit space is developed by DSV. Furthermore, DSV was obtained in this study by correlating the subjective satisfaction with the daylight environment and the horizontal illuminance level. Section 2.2 details the development of the DSV formula.

2.1.3. Artificial neural network (ANN)

Artificial intelligence was an effective and feasible tool to generate the prediction model. Many researches [33–36] had applied the Artificial Neural network (ANN) in the field of daylighting simulation over the last few years and achieved good performance. As an illustration, Nault et al. [34] acquires the dataset through the daylight simulation of parametric modeling and modeled by the multiple linear regression to predict the spatial daylight autonomy (sDA). In addition, some researches [37,38] combine the ANN into the optimization of shading strategy and present a model that can make the parametric modeling faster.

2.1.4. Multi-objective genetic algorithm (MOGA)

This study addressed a multi-objective problem with two objectives that change in opposite directions, so its solution was not unique. A solution that is not dominated by another is called a nondominated solution, and the group of nondominated solutions

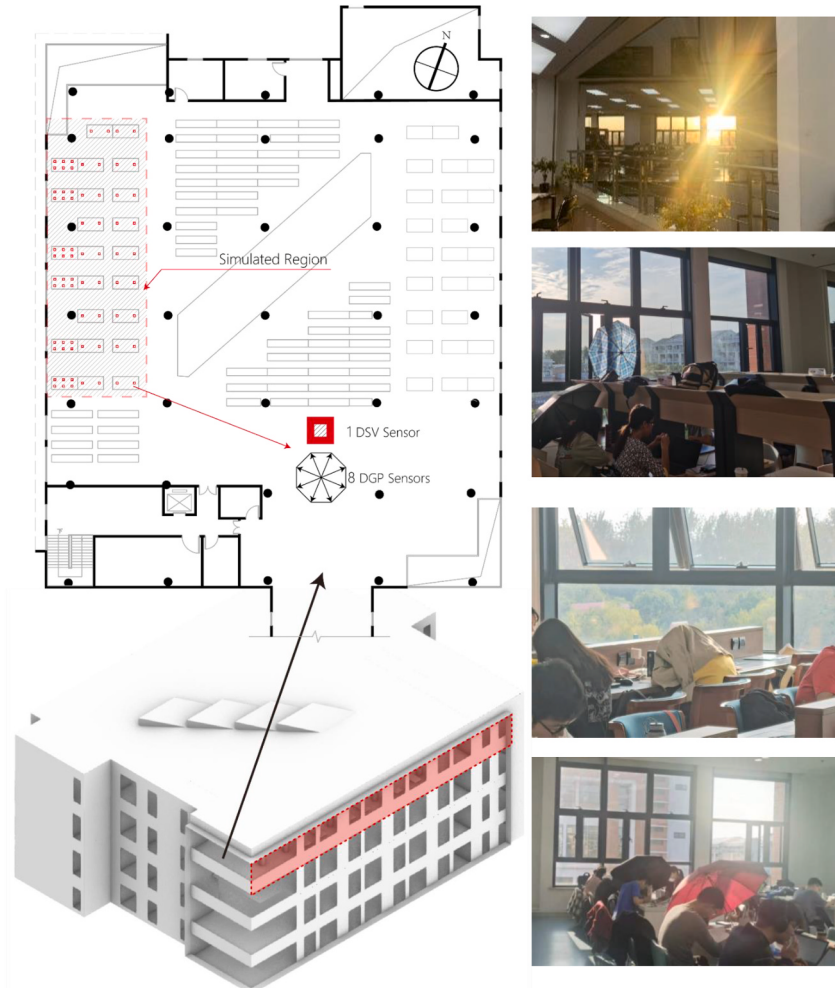


Fig. 2. The studied library, plan of the studied area, virtual test points of DSV, DGP, and photos showing actual conditions.

generated in the optimized algorithm is called a Pareto set [39,40], which can be obtained by the MOGA. In the MOGA process, the first-generation parameters of the shading device are randomly set, and the Pareto set is empty. Next, these nondominated individuals are together assumed to constitute the first nondominated front with a large fitness value [41], where the fitness combines SGA0.35/95% with sDVA0.30/80%. In the optimized process, if the new solution generated by the optimization process is not dominated by another nondominated solution, it replaces the dominated individuals in the original Pareto set or is deposited directly into the Pareto set. The MOGA produces a final Pareto set when the generation reaches the pre-set generation.

The MOGA used in this study was the nondominated sorting genetic algorithm-II (NSGA-II) in the Wallacei X package of the Grasshopper plugin. Wallacei optimizes the objective function to a minimum value, and when the objective function needs to be maximized, the input objective values should be transformed into complementary values. Recently, the NSGA-II algorithm is frequently used by building environment and energy researchers to achieve a balance between energy consumption and occupants' satisfaction [42,43].

2.2. Correlating horizontal illuminance with daylight subjective vote (DSV)

Many previous studies have employed useful daylight illuminance (UDI) [44] as one of the objective functions to optimize the parameters of shading devices [11,17,20,23,42]. UDI assumes that occupants are satisfied with the daylight environment under a reasonable illuminance range. However, Handina et al. [45] pointed out that occupants' perceptions of the daylight environment did not change consistently with UDI, while Hu et al. [46] found that eye fatigue first decreased and then increased as illuminance increased from 0 lux to 1300 lux, and the lowest perception of fatigue was at 700 lux. In other words, UDI assumes the same satisfaction within a certain range of illuminance, but people's actual perception varies with the illuminance level. The same is true for indices such as daylight autonomy (DA) [30]. To provide a more accurate assessment, the present study first developed a formula to correlate subjective satisfaction with the illuminance level, and then used the developed formula as the basis of the objective function.

To develop the formula, this study conducted field surveys in the reading areas of a university library and asked occupants about their satisfaction with the daylight environment, while the horizontal illuminance level was measured simultaneously at desk height. Using the questionnaire designed by Ref. [47], we asked the occupants to vote on their subjective level of satisfaction with the daylight environment according to the five scales (1, 0.75, 0.5, 0.25, 0), where smaller values indicated higher satisfaction. The other sections of the questionnaire were not directly related to the current study, so they are not discussed here. The field survey was conducted 5 times between 9:00 and 17:00 during the period from January 1 to May 30, 2021, and a total of 606 samples were collected. The dataset was then used to develop a relationship between horizontal illuminance level and subjective satisfaction with the daylight environment.

2.3. Case study

2.3.1. Studied building

Our method for optimizing and selecting a shading strategy was applied to a university library in Shanghai, China ($W121.433^\circ$, $N31.028^\circ$). We chose the west side of the top (fourth) floor of the studied region because it was exposed to very strong sunlight in the afternoon due to the very high glazing ratio (42.6%) in the western façade. The floor plan of the test region is provided in Fig. 2, along with photos of existing conditions. Occupants used umbrella and clothes as adaptive measures against the excessive sunlight. Test points for DSV and DGP were arranged in the reading area on the west side of the building, as shown in Fig. 2. In addition, we set eight radial directional DGP sensors for one test point and one DSV sensor for one test point (576 DGP sensors and 72 DSV sensors), where the multi-directional sensors of DGP were set up to take into account the glare sources from all directions of the daylit space. The simulation was conducted during daylight hours for an entire year and the sky condition is decided by the weather file.

This study uses the artificial neural network (ANN) to effectively get the objective function and sets a greater space for optimization, specifically, we set the population size, population generation, mutation rate, and crossover rate as 50, 100, 0.33, and 0.9, respectively. It took approximately 100 ms to analyze each "individual", and the calculation of all generations took approximately 10 min. The ANN was built by the lunchbox tools in grasshopper, which provides diverse learning algorithms and activation functions to choose from. Meanwhile, the dataset was divided into training data and test data, where the split rate of test data is 0.15. The dataset is the result of the daylight simulation of the study case by radiance. Table 2 shows the specific parameters in the daylight simulation.

2.3.2. Shading strategies

To remedy the poor existing window design, four shading strategies, namely, perforated aluminum sheet (PAS), vertical slats (Vs), serrated windows with southern orientation (Sw_S), and serrated windows with northern orientation (Sw_N), were selected for optimization and comparison. Fig. 3 shows the four strategies and the corresponding design variables. Perforated aluminum sheet changes the window-to-wall ratio to prevent glare and at the same time changes the distribution of daylight. PAS can efficiently control excessive daylight and increase useful annual daylight [48]. The number and size of the holes in the PAS are the key parameters of shading effectiveness. As a result, the design variables of the PAS are the number of holes in the vertical and horizontal columns and

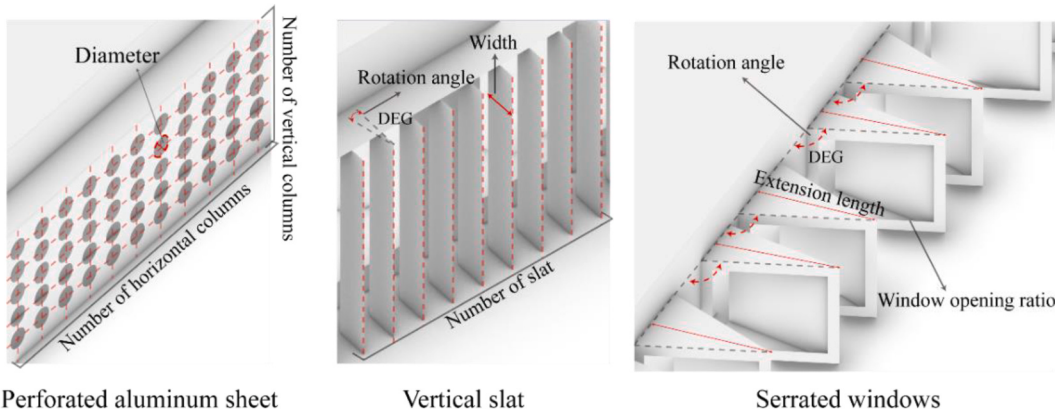
Table 2
Glare ratings for different DGP ranges.

Ranges of DGP	Glare rating
0.35 > DGP	Imperceptible glare
0.35 < DGP < 0.4	Perceptible glare
0.4 < DGP < 0.45	Disturbing glare
0.45 < DGP	Intolerable glare

Table 3

The boundary condition of daylighting simulation.

Daylight Simulation information	Boundary condition
Wall reflectance	0.7
Windows transmittance	0.65
Ceiling reflectance	0.7
Floor reflectance	0.3
Mesh grid size	0.6 m, 0.8 m
Distance to move sensors from the floor surfaces	0.7 m
Number of radial directions for DGP sensors for one simulated point	8(22.5, 67.5, 112.5, 157.5, 202.5, 247.5, 292.5, 337.5)
Number of DSV sensors for one simulated point	1
Simulated period	Annual for each hour
Radiance parameters	-ab 2 -ad 5000 -lw 2e-05
Location (Weather file)	Shanghai

**Fig. 3.** Four studied shading strategies and corresponding design parameters, where the serrated windows represent the different shading strategies of Sw_S and Sw_N.

also the hole diameters.

When vertical slats are used, the angle of the slats can be adjusted to obstruct most daylight from directly entering the room. Lee et al. [49] considered Vs to be the best shading device among vertical louvers, horizontal louvers, eggcrate louvers, overhangs, vertical slats, horizontal slats, and light shelves for improving UDI at the east and west orientations. The design variables of Vs are the number, width, and rotation angle of the slats.

Serrated windows transform the received sunlight from direct to diffuse by alternating the orientation of the windows [50–52]. In this study, the Sw “changes” the facade orientation from west to south, to avoid the direct afternoon sunlight from the west while taking advantage of the diffuse sunlight from the south or north. The Sw with southern is contributed to reducing the glare from the western sun, but it is also restricted the sunlight directly into indoors. Compared to the Sw with southern, the opposite is true for Sw with northern. To more accurately research the shading strategy, we separately set the opening surface in the opposite direction, namely, one was the serrated windows facing south (Sw_S) and the other one is the serrated windows facing north (Sw_N). The design parameters of the Sw are the rotation angle, extension length, and window opening ratio of the blocking surface.

For modeling the artificial neural network, according to the characteristic of the shading device, we set the adequate data format. The input data of ANN is the parameter of the shading device, and the output result of ANN is the daylight performance with the shading device, namely, sGA0.35/95% with sDVA0.30/80%. To capture as much of the performance of the shading device, we set a

Table 4

Artificial Neural Network inputs.

Shading strategy	Input variables	Boundary condition	Range	Train steps	Train quantity	Test steps
PAS	Vertical columns	Generic	(3-20)	2	8	1
	Horizontal columns	Reflectance 0.35	(9-80)	8	9	1
	Hole diameters		(0.1-0.5 m)	0.05	10	0.001
Vs	Rotation angle	Generic	(-0.48-0.42π)	0.1	10	0.001
	Slat width	Reflectance 0.35	(0.1-1.9 m)	0.2	10	0.01
	Slat number		(10-80)	10	8	1
Sw	Rotation angle	Generic	(-1.5-1.9π)	0.4	11	0.001
	Extension length	Reflectance 0.35	(0.3-4.8 m)	0.5	10	0.01
	Hole ratio		(0.1-0.95)	0.1	9	0.01

reasonable variable range for every parameter. We then use the method of quadrature sampling to obtain the training input data, and capture the correspondingly training output data by daylighting simulation. Table 4 shows the specific setups of training and testing sampling.

3. Results

This section first presents the formula that was developed for the prediction of subjective satisfaction with the daylight environment using the horizontal illuminance level. Next, the result of training an artificial neural network (ANN) and the daylight performance of the original environment are shown. Finally, the optimization of the four shading strategies is described, and the strategies are compared.

3.1. Daylight subject vote (DSV) formula

A formula was developed from the surveyed data to correlate the daylight subjective vote (DSV) with the horizontal illuminance level. According to ISO 8995 [53], the data was first “binned” into (150,200], (200,300], (300,500], (500,750], (750,1000], (1000, 1500], (1500,2000], (2000,3000], (3000,5000], (5000,10000], (10000,15000], (15000,20000], (20000,25000] and (25000, -] intervals of illuminance. Next, the mean DSV value for each bin was calculated; these values are presented in Fig. 4. Because the illuminance level increased much faster than the change in the occupants’ DSV, the x-axis was transformed logarithmically, as is commonly practiced in daylighting research [54]. It can be seen that the satisfaction was high at an illuminance of around 1000 lux, but decreased when the illuminance became higher or lower. A quadratic function was used to correlate the DSV with the logarithmic illuminance (E_h , lux), as shown in Equation (5). The obtained equation was then used in the objective function to calculate the DSV with the simulated illuminance.

$$DSV = 0.003025[2.4098 \ln(E_h) - 10.233]^2 - 0.0405[2.4098 \ln(E_h) - 10.233] + 0.380175 \quad (5)$$

While the occupants’ vote value is used to develop the correlation between desktop illuminance and occupants’ perception, the final satisfaction ratings of satisfactory, neutral, unsatisfactory, and very unsatisfactory levels of DSV were determined by corresponding illuminance ranges according to Refs. [44,53,55,56]. The satisfactory illuminance range was 500–2000 lux, the neutral illuminance ranges were 200–500 lux and 2000–5000 lux, the unsatisfactory illuminance ranges were 100–200 lux and 5000–10000 lux, and the very unsatisfactory illuminance ranges were lower than 100 lux or greater than 10000 lux. Table 5 determined the corresponding ranges of DSV for specific satisfactory levels.

3.2. Artificial neural network (ANN) results

An artificial neural network enables fast acquisition of dynamic daylight performance with the shading device. Table 6 shows the specific setups for different ANN models and the accuracy of the pre-trained model on the test dataset. It can be seen that R^2 , root mean square error (RMSE), and mean absolute error (MAE) between test data and predicted data have a good fit, as shown in Fig. 5.

3.3. Original daylight environment

In this section, the performance of the original daylight environment was simulated and displayed by the hourly spatial average of daylight subjective vote (DSV) and daylight glare probability (DGP) throughout the entire year. Fig. 6(a) shows the hourly DSV for an entire year for the original daylight environment without any shading devices. From a year-round perspective, DSV was lower in the

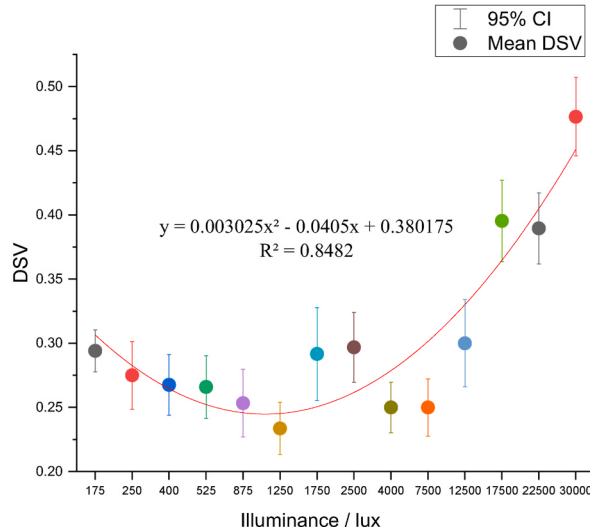


Fig. 4. Relationship between DSV and horizontal log illuminance.

Table 5

Satisfaction ratings for different DSV ranges.

Ranges of DSV	Satisfaction rating
0.25 > DSV	Satisfactory
0.25 < DSV <0.3	Neutral
0.3 < DSV <0.35	Unsatisfactory
0.35 < DSV	Very unsatisfactory

Table 6

Partitioning of training and validation datasets and the specific settings of the artificial neural network.

Train setup and results							Test results			
Training tasks	# of Train dataset	# of Test dataset	Hidden neurons	Learning Algorithm	Activation Function	Epoch	MSE	R ²	RMSE	MAE
sGA of PAS	612	108	18	A1	B1	1300	5.2e-6	0.985	7.6e-3	3.4e-3
sDVA of PAS	612	108	16	A2	B0	760	4.8e-6	0.985	1.2e-2	3.6e-3
sGA of Sw_N	841	149	20	A1	B1	1300	4.78e-7	0.996	7.0e-3	4.1e-3
sDVA of Sw_N	841	149	12	A2	B0	760	2.36e-6	0.985	1.6e-2	7.1e-3
sGA of Sw_S	841	149	20	A2	B2	1300	1.0e-5	0.998	7.3e-3	4.1e-3
sDVA of Sw_S	841	149	12	A0	B2	760	7.9e-5	0.983	1.1e-2	4.2e-3
sGA of Vs	680	120	21	A0	B1	1500	1.8e-5	0.947	6.2e-2	3.8e-2
sDVA of Vs	680	120	21	A0	B1	1300	5.3e-5	0.946	6.3e-2	4.6e-2
Data Division	Random, split rate = 0.15									

Learning Algorithm: A0 = Backpropagation; A1 = Evolutionary algorithm; A2 = Levenberg-Marquardt;**Activation Function:** B0 = Sigmoid; B1 = Bipolar Sigmoid; B2 = Linear;**Loss function:** MSE = Mean Square Error; R² = The coefficient of determination; RMSE = Root Mean Square Error; MAE = Mean Absolute Error;

period 8:00 a.m. to 2:00 p.m. of spring (March to May) and summer (June to August), and relatively higher in the period (3:00 p.m. to 6:00 p.m.). The DSV performance was determined by the illuminance levels, and natural illuminance levels are related to solar intensity. It can be deduced that the intensity of sunlight from 8:00 a.m. to 2:00 p.m. was appropriate and did not shine directly into the interior space. In autumn (September to November) and winter (December to February), the satisfaction levels were higher than those in spring and summer.

The distribution of hourly DGP for an entire year in the original daylight environment was present in Fig. 6(b). It is obvious that the perceptible, disturbing and intolerable glare levels in the west-facing spaces were distributed between 12:00 and 6:00 p.m., while most of the imperceptible glare was during the morning hours.

Fig. 6(c) shows the distribution of different satisfaction levels of DSV in the original daylight environment. The ratio of unsatisfactory and very unsatisfactory levels was nearly 20%. It was confirmed that the presence of too high and too low illuminance levels in the original daylight environment caused high DSV value and dissatisfaction. Fig. 6(d) illustrates the DGP distribution for each glare level in the original daylight environment. The perceptible disturbing, and intolerable glare accounted for more than 20%. The percentage of intolerable glare accounted for more than half of the glare with DGP >0.35.

3.4. Optimization of shading strategies

The optimization results for the four strategies, including perforated aluminum sheet (PAS), vertical slats (Vs), serrated windows facing south (Sw_S), and serrated windows facing north (Sw_N), are discussed in this section, where the MOGA optimization, the final Pareto set, and the daylight environment of the near-optimal shading device for each strategy are presented and compared.

3.4.1. Perforated aluminum sheet (PAS)

The optimization process led to a Pareto set with 848 solutions for the PAS strategy. The complementary sGA0.35/95% with complementary sDVA0.30/80% values for the 848 solutions are shown in Fig. 7. The performance of the original environment (complementary sGA0.35/95% = 0.45, complementary sDVA0.30/80% = 0.42) without the application of any shading strategies was also displayed in Fig. 7. The complementary sGA0.35/95% values for the 848 optimized solutions were all smaller than the values for the original performance. Thus, the PAS can effectively reduce glare. However, only 65 solutions had better performance than the original design in providing a dynamic satisfactory illuminance level. These solutions with better performance are enclosed in a red box in Fig. 7. A near-optimal solution that provided the maximum reduction of sGA0.35/95% while retaining the same sDVA0.30/80% with the original space was then identified and is shown in yellow.

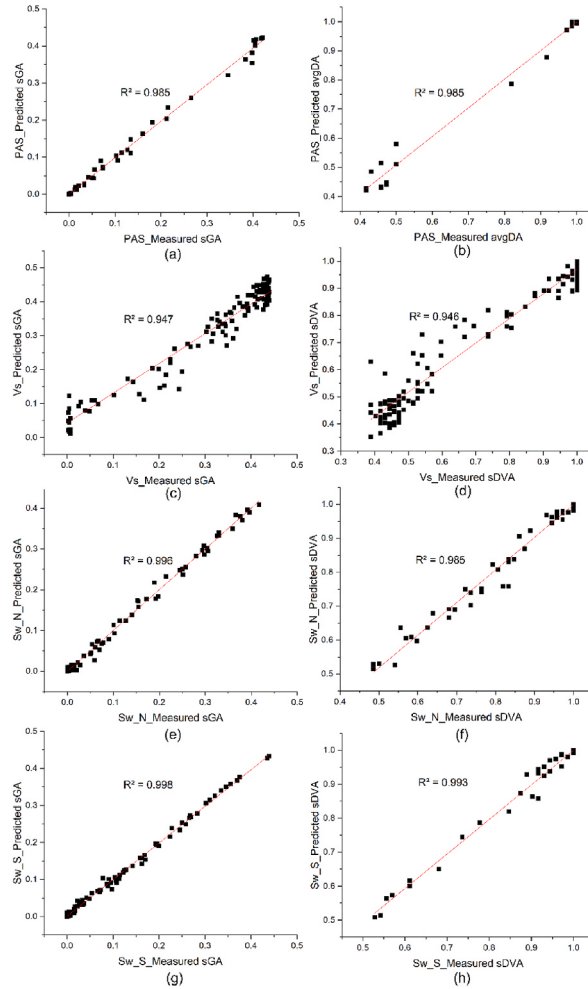


Fig. 5. The fitting accuracy of artificial neural network for the daylight environment with PAS, Vs Sw_N and Sw_S.

To demonstrate the glare reduction effect, Fig. 8(a) shows the distribution of DGP from a whole year for the near-optimal PAS. Most perceptible, disturbing, and intolerable glare levels occurred between 1:00 p.m. and 6:00 p.m. Furthermore, the DGP in the autumn and winter months had a relatively narrow distribution, but the DGP values often exceeded the intolerable level of 0.45. It can be deduced that the near-optimal PAS blocked the afternoon glare when the sun elevation was high during the spring and summer months, but in autumn and winter, the low-angle sun could still pass through the holes and cause glare. Fig. 8(b) displays the distribution for each glare level of DGP in the daylight environment with the near-optimal PAS. Overall, the imperceptible and perceptible glare levels accounted for nearly 90% of the simulated period.

3.4.2. Vertical slats (Vs)

Fig. 9 shows the Pareto set of the Vs, which had 429 solutions after optimization. All solutions of the Pareto set had a better sGA than the daylight environment without a shading device. Thus, the Vs effectively reduced the glare. Although these nondominated solutions reduced the glare, only 68 of the solutions displayed in red had better sDVA performance than the original environment. Considering the practical needs of occupants, a near-optimal solution is shown in yellow, with similar sDVA to the original environment, while maximally reducing the glare.

Fig. 10(a) displays the distribution of hourly DGP for an entire year for the near-optimal Vs. We can see that most of the perceptible glare was occupied in the afternoon (1:00 p.m. to 5:00 p.m.) of autumn and winter months. This implies that the slats of the near-optimal Vs efficiently reduced the glare from the low solar angle during the autumn and winter months. Fig. 10(b) shows the distribution of different glare levels of DGP in the daylight environment with the near-optimal Vs. The ratio of disturbing and intolerable glare levels was lower than 8%. The near-optimal Vs blocked most of the glare and improved visual comfort, as compared with the original environment.

3.4.3. Serrated windows facing north (Sw_N)

For the performance of the serrated window, we first examined the north-facing windows (Sw_N). The optimization of Sw_N

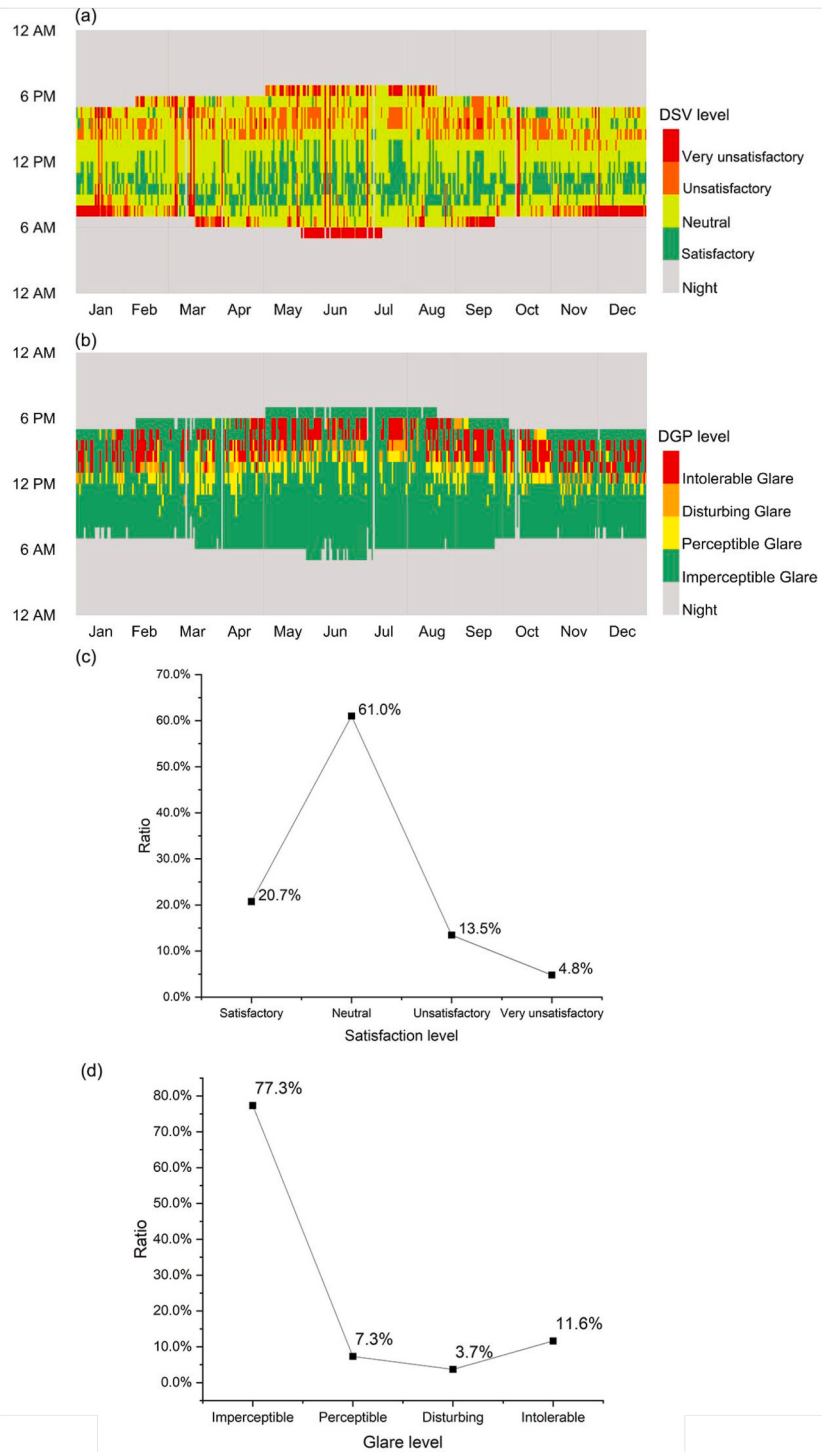


Fig. 6. The distribution of DSV and DGP for the original daylight environment: (a) the DSV from 1/1 to 12/31 for a daylit time in the daylight environment, (b) the DGP from 1/1 to 12/31 for a daylit time in the daylight environment, (c) the ratio for each satisfaction level, and (d) the ratio for each glare level.

resulted in 547 nondominated solutions in the Pareto set. The complementary sGA0.35/95% and complementary sDVA0.30/80% of all the nondominated solutions are shown in Fig. 11. All solutions in the Pareto set exhibited a lower DGP than that of the original daylight environment. As indicated by the DGP performance, the Sw_N can effectively reduce glare, and the optimization of Sw_N was productive. However, no solutions provided greater satisfaction with the daylight environment than the situation without any shading

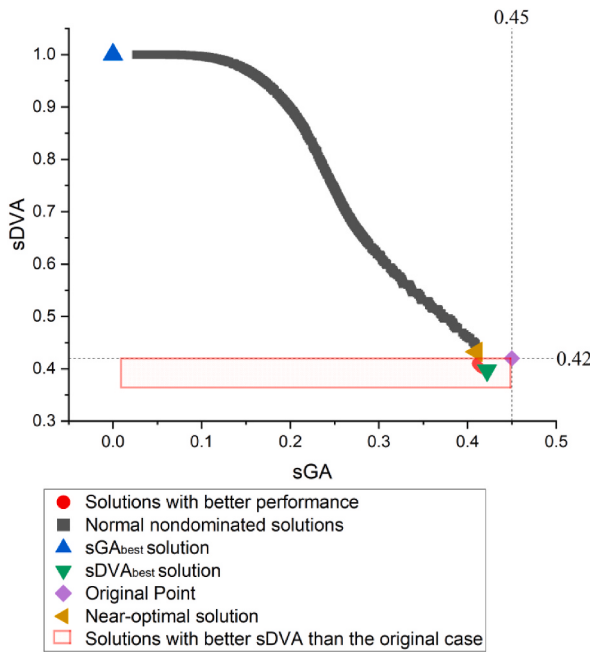


Fig. 7. The Pareto set of PAS, the solution of the original performance, solutions with better performance than the original one, the solution of best sGA and best sDVA, and the near-optimal solution in the Pareto set.

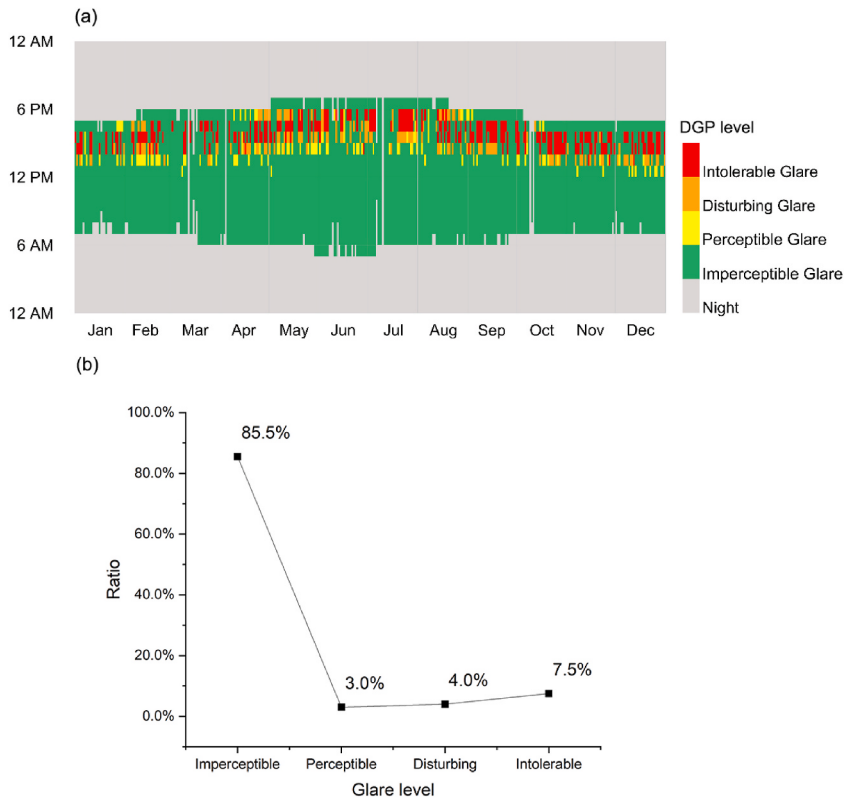


Fig. 8. The distribution of DGP for the near-optimal PAS: (a) from 1/1 to 12/31 for a daylit time in the daylight environment, and (b) the ratio for each glare level.

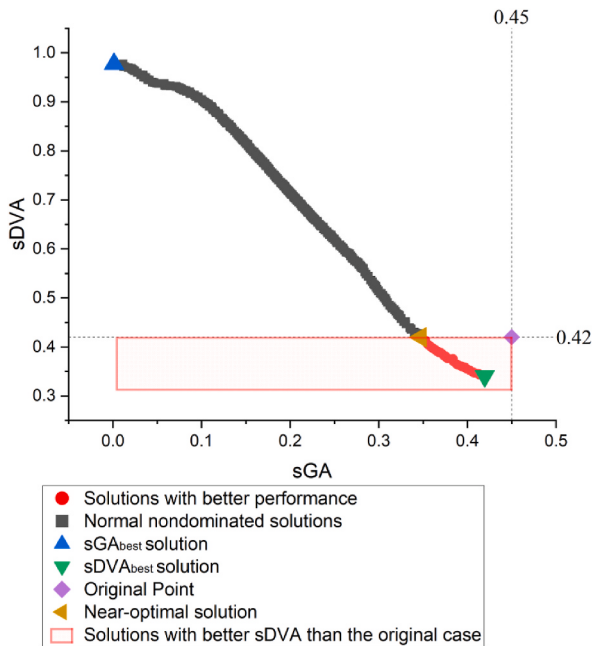


Fig. 9. The Pareto set of Vs, the solution of the original performance, solutions with better performance than the original one, the solution of best sGA and best sDVA, and the near-optimal solution in the Pareto set.

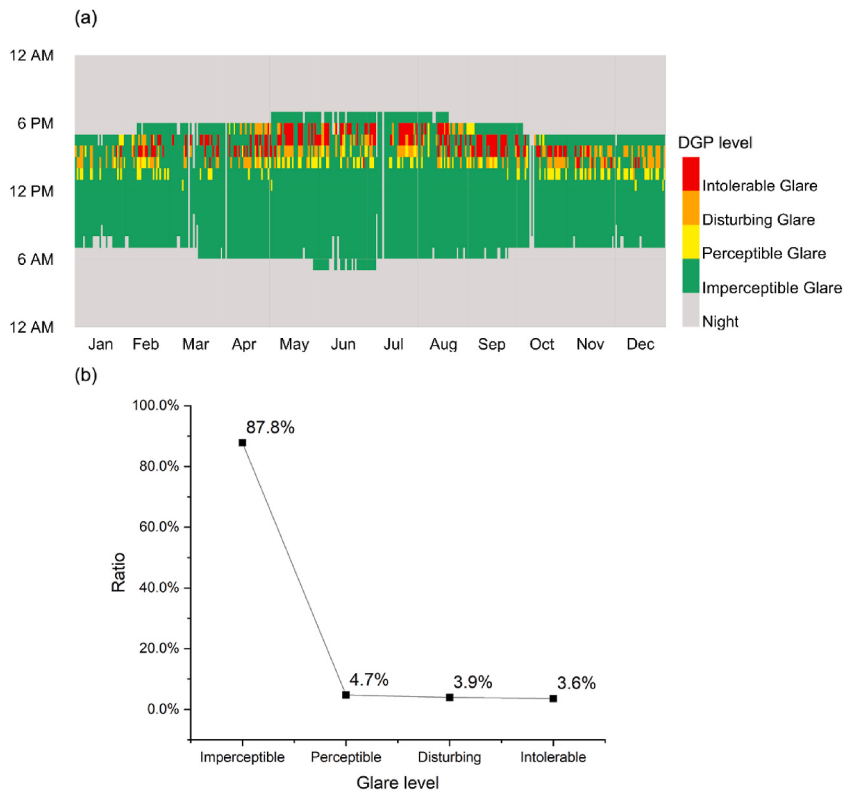


Fig. 10. The distribution of DGP for the near-optimal Vs: (a) from 1/1 to 12/31 for a daylight time in the daylight environment, and (b) the ratio for each glare level.

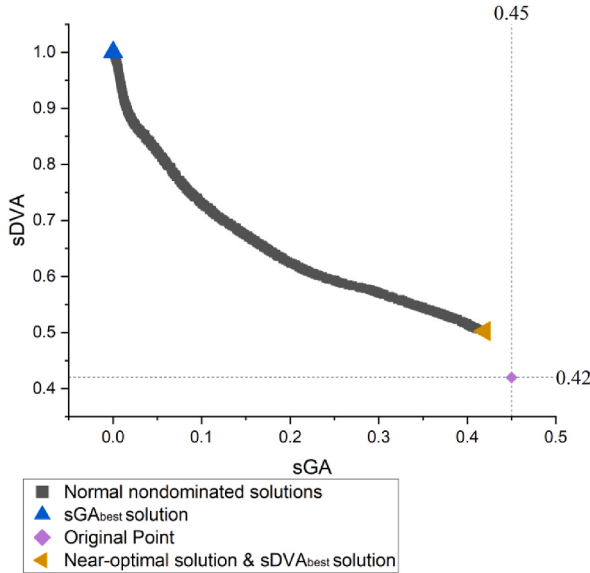


Fig. 11. The Pareto set of Sw_N, the solution of the original performance, the solution of best sGA and best sDVA, and the near-optimal solution in the Pareto set.

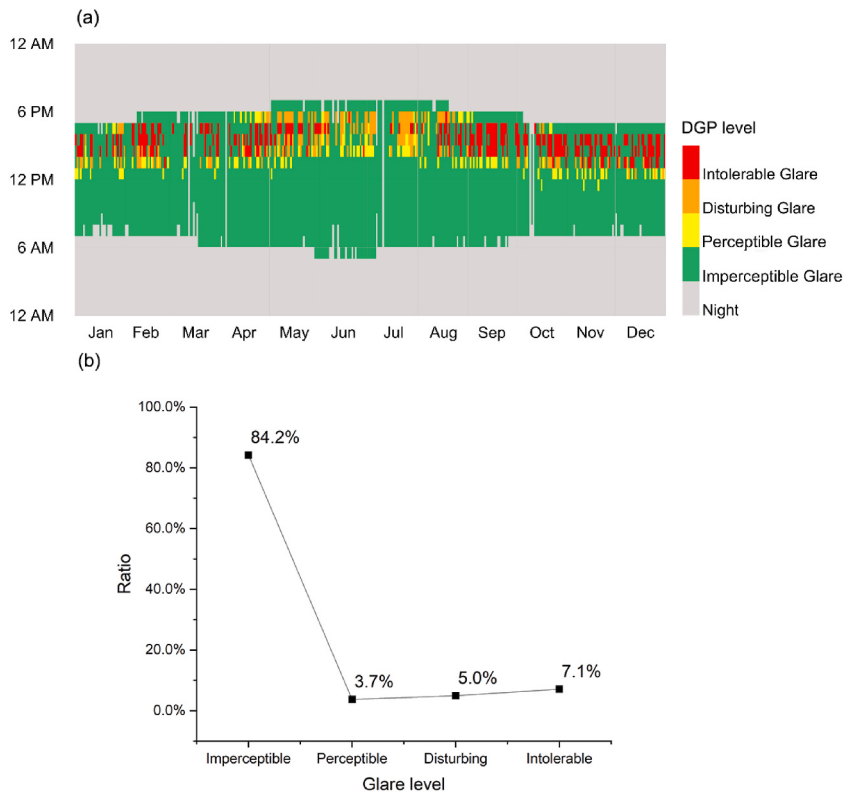


Fig. 12. The distribution of DGP for the near-optimal Sw_N: (a) from 1/1 to 12/31 for a daylit time in the daylight environment, and (b) the ratio for each glare level.

device. For maintaining the satisfaction level, the solution with the greatest satisfaction was set as the near-optimal solution.

Fig. 12(a) displays the distribution of hourly DGP for an entire year in the daylit space with the near-optimal Sw_N. During the whole day, it was obvious that the perceptible, disturbing, and intolerable glare levels almost took place during the period (1:00 p.m. to 6:00 p.m.). The spring, autumn, and winter days were mostly dominated by disturbing and intolerable glare during this time (1:00 p.m. to 6:00 p.m.). This was because the blocking surface of Sw_N can't impede most of the = low-angle sunlight during which spring,

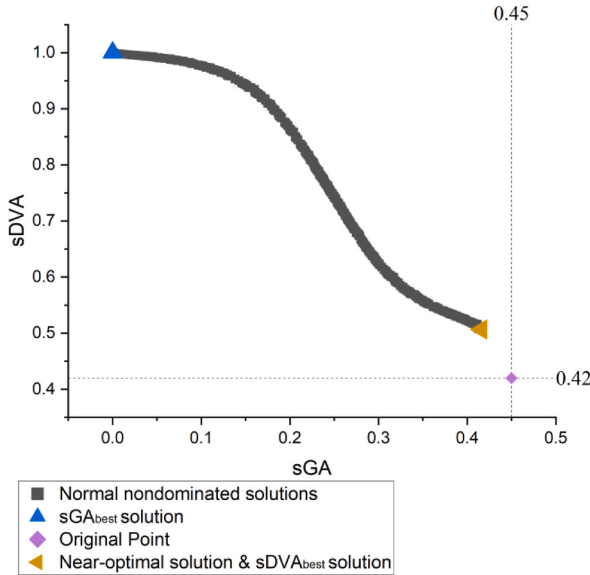


Fig. 13. The Pareto set of Sw_S, the solution of the original performance, the solution of best sGA and best sDVA, and the near-optimal solution in the Pareto set.

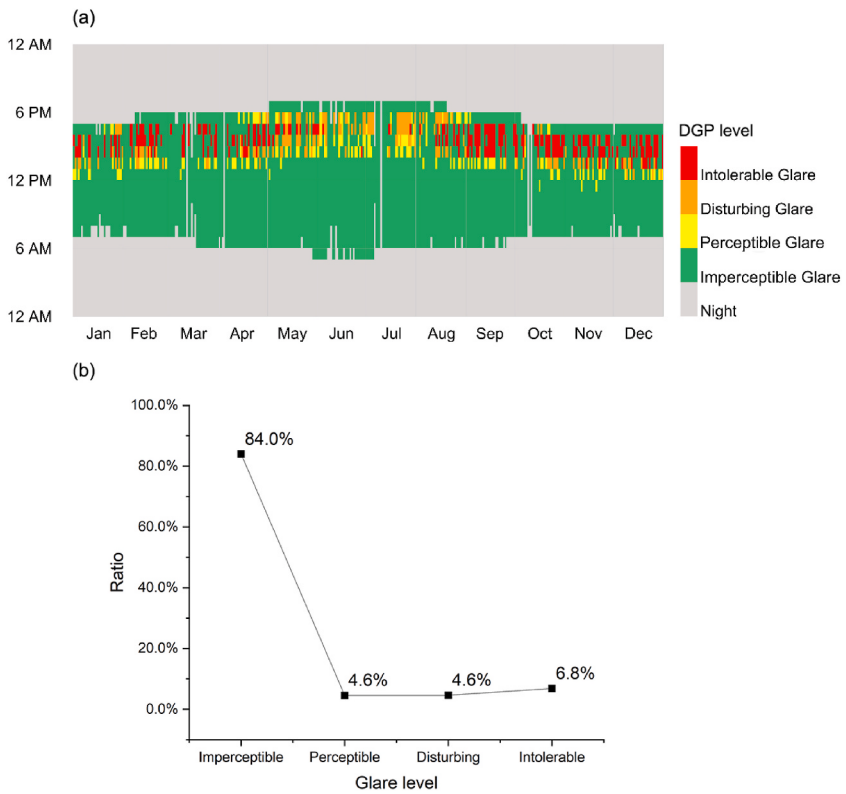


Fig. 14. The distribution of DGP for the near-optimal Sw_S: (a) from 1/1 to 12/31 for a daylit time in the daylight environment, and (b) the ratio for each glare level.

autumn, and winter months. Fig. 12(b) shows the distribution of DGP for each glare level in the daylight environment with the near-optimal Sw_N. The perceptible, disturbing, and intolerable glare levels accounted for more than 15% of the investigated period.

3.4.4. Serrated windows facing south (Sw_S)

Fig. 13 displays the Pareto set of Sw_S, which had 782 nondominated solutions after optimization. All nondominated solutions can effectively reduce glare. The optimization of Sw_S was productive, but the solution did not well balance glare reduction and

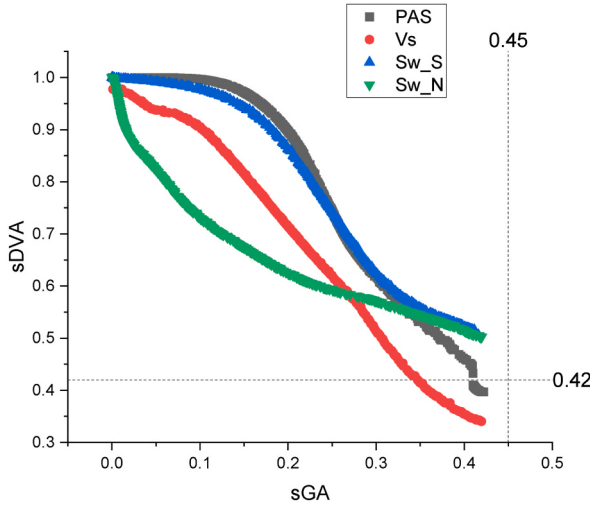


Fig. 15. Comparison of the Pareto sets for Sw_N, Sw_S, Vs, and PAS.

illuminance maintenance: all solutions had a worse performance than the original performance. The solution with the greatest DSV satisfaction was selected as the near-optimal solution.

Fig. 14(a) displays the annual DGP distribution for the near-optimal Sw_S. As reflected by the change in DGP, the daylight environment for the near-optimal Sw_S provided a stable and comfortable daylight environment on typical summer days. Furthermore, the glare occurred and ended earlier in autumn and winter than in spring and summer. This represents that sunlight at lower angles can enter the room earlier and sunset is also earlier in the autumn and winter. **Fig. 14(b)** displays the proportion of different glare levels for the near-optimal Sw_S. The percentage of imperceptible and perceptible glare levels accounted for nearly 90%.

3.5. Comparison of the four shading strategies

Fig. 15 compares the Pareto sets for the four shading strategies, namely, the perforated aluminum sheet (PAS), vertical slats (Vs), serrated windows facing north (Sw_N), and serrated windows facing south (Sw_S). As displayed in **Fig. 15**, Sw_S and PAS had a relatively bad performance for both spatial glare autonomy (sGA) and spatial daylight vote autonomy (sDVA). The Pareto sets for the PAS and Sw_S coincided with each other for complementary sGA0.35/95% values between 0.25 and 0.33, indicating that the two strategies had similar performance in that range. Furthermore, Sw oriented to the north performed better than that oriented to the south. The university library has turned about 20° to the east, which resulted in much more sunlight exposure from the south.

In areas where complementary sGA0.35/95% was lower than 0.27, the Sw_N had lower, and thus better, complementary sDVA0.30/80% values than the Vs. This finding implies that the Sw_N can provide better illuminance levels than the Vs in areas with low glare. In the areas where complementary sGA0.35/95% was greater than 0.27, Vs has better daylight performance than other shading strategies. In the areas where complementary sGA0.35/95% was greater than 0.33, PAS has better daylight performance than Sw_N and Sw_S, where Sw_S and Sw_N had a similar performance “curve”.

While the complementary sGA0.35/95% for the near-optimal PAS, Vs, Sw_S, and Sw_N were significantly lower than in the original case, the complementary sDVA0.30/80% remained relatively unchanged, as shown in **Fig. 16**. **Fig. 16(a)** compares the ratio for each satisfaction level among the four near-optimal shading devices and the original design. The ratio was similar for these five cases in unsatisfactory and very unsatisfactory levels. At the satisfactory level, the original ratio was slightly greater than Sw_N and Sw_S for the near-optimal shading devices, while Vs and PAS of the near-optimal devices had a greater ratio than the original case. This result implies that PAS and Vs of the near-optimal device efficiently block the sunlight during periods of high solar intensity, resulting in a better satisfaction level. While Sw_N and Sw_S of the near-optimal device excessively obstruct the sunlight, resulting in a worse satisfaction level.

Fig. 16(b) shows the ratio of all glare levels for the four near-optimal shading strategies. The ratio of all glare levels for the original case is also displayed for comparison. Overall, the near-optimal PAS, Vs, Sw_N, and Sw_S greatly reduced the complementary sGA0.35/95%, by 9%, 22%, 8%, and 8%, respectively, when compared to the original complementary sGA0.35/95%. The near-optimal Vs exhibited the best performance in complementary sGA0.35/95% reduction. In addition, each test point had eight DGP sensors which different orientations, where the sensors viewing for indoor occupied half ratio. Therefore, the percentage of glare was reduced to a relatively low level. If only the sensors of DGP for which glare occurs were considered, the numerical ratio of glare reduction for each shading device would be twice or more.

4. Discussion

4.1. Application of artificial neural network for maximum mining the performance of shading strategy

While comparing the performance of shading strategies, the setups of boundary conditions were important. For obtaining the fullest

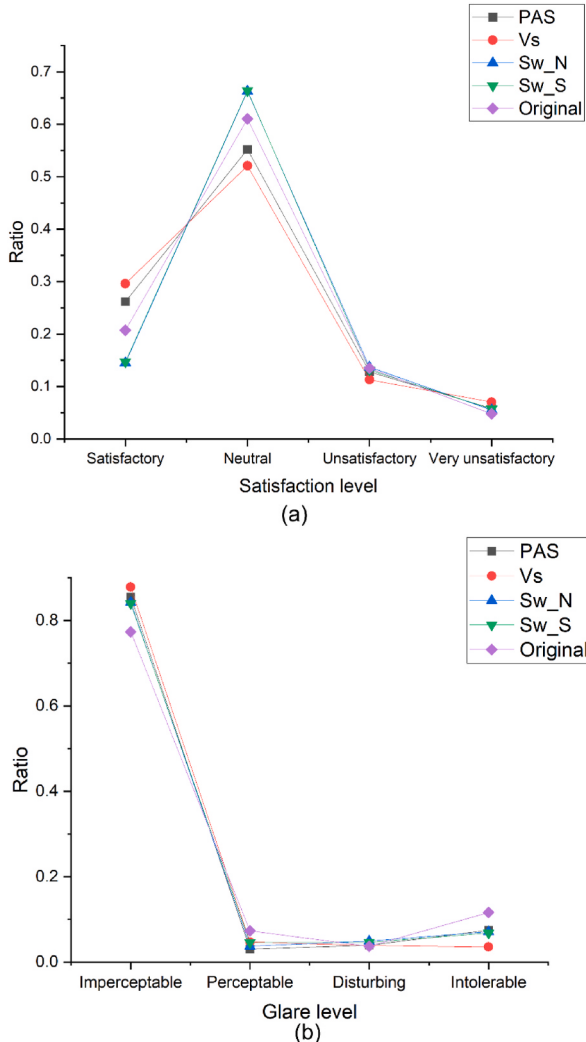


Fig. 16. The comparison of the ratio of all satisfaction levels (a) and all glare levels (b) for the original case and the near-optimal solutions for Sw_S, Sw_N, Vs, and PAS, respectively.

possible daylight performance, a large number of numerical experiments should be conducted to find the parameters of best and worst daylight performance for each shading strategy. The artificial neural network (ANN) was applied to reduce the simulation time. This study used limited computing resources (i7-8700K CPU @3.7 GHz). The simulation and data processing of the 72 sensors of illuminance and the 576 sensors of DGP by radiance for an entire year took about 2 min for one “individual”. All searching quantities are 5000 in the multi-objective genetic algorithm process, and would take approximately 10000 min (about 167 h). By using the ANN to model the DSV and DGP, one “individual” search was reduced to 100 ms and the consuming time of all parametric searching was about 10 min. In addition, the ANN predictions preserved high accuracy, as evidenced by the result that the coefficient of determination (R^2) is higher than 0.94 in all tasks (Fig. 5). In addition, the greater parametric searching space and larger scale (temporal and spatial) simulation can maximumly mine the performance “curve” (Pareto set) for each shading strategy to conduct the comparisons of daylight performance.

4.2. The principle of the shading strategy

The shading strategy reduces the glare and maintains a satisfactory level in the daylit space by blocking direct sunlight or diffusing direct sunlight into indoors. Therefore, the design of the shading surface is very important for each shading strategy. In this study, we compared four shading strategies, where the shading design and the result of the comparison as shown in Figs. 3 and 15, respectively. We then found a dramatic difference in daylight performance between the four shading strategies, especially Vs and Sw_N had a better daylight performance than PAS and Sw_S. The performance gap for each shading strategy could be explained by the shading design of blocking and diffusing direct sunlight. We choose the 3:00 p.m. on 24 January to conduct the analysis of shading principles for four strategies, and the sun path in the time is shown in Fig. 17 (a). Fig. 17 (b) shows PAS blocks a part of direct sunlight by the unperforated

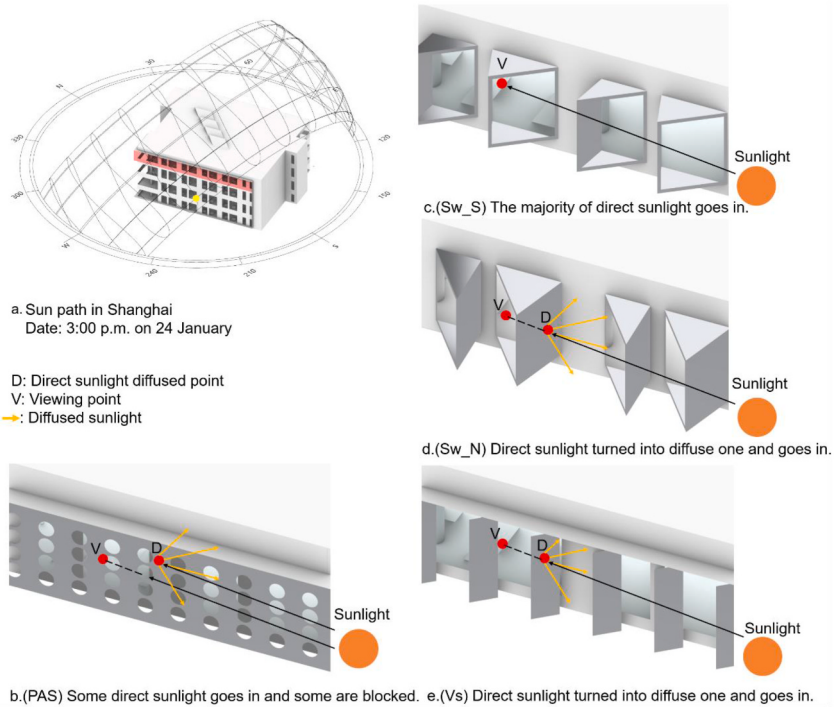


Fig. 17. The sun path in Shanghai at 3:00 p.m. on 24 January (a), the shading diagram of (b) PAS, (c) Sw_S, (d) Sw_N, and (e) Vs, respectively.

surface, but it lacks the characterizer of diffusing direct sunlight and the glare may be happened by the sunlight through the hole. Sw_S almost couldn't block the sunlight from the south to the west, and it worked until the sun fully move to the west which was nearly sunset, the diagram as shown in Fig. 17 (c). On the contrary, Fig. 17 (d) displays Sw_N could block the direct sunlight from the south to the west by the south shading surface, and the shading surface also could diffuse some sunlight into the abut window to maintain the reasonable illuminance level. As shown in Fig. 17 (e), the diagram of shading principles for Vs, where the slat of Vs reflects the direct sunlight to the abut slat or indoor space to reduce glare.

4.3. Limitations

Our case study shows the multi-objective genetic algorithm can provide continuous and comprehensive performance curves, and thus was very effective for comparing different shading strategies. However, limitations exist. Shading design not only impacts visual comfort but also has significant effects on thermal comfort, the occupants' view, and building energy consumption. In addition to blocking light, shading prevents solar heat from entering the building and impedes the occupants' views to outside environment. Although this study was focused only on the daylight environment, the design method proposed can also be applied to the optimization of the shading strategy in terms of solar-related thermal comfort, building energy consumption, and occupants' view. Our study proposed a formula to correlate illuminance with subjective daylight satisfaction based on the analysis of field survey data. However, this formula may not be accurate under low illuminance levels, since the data was collected during normal working hours on sunny days when the illuminance was above 150 lux.

5. Conclusions

Many shading strategies are available to control unwanted glare, but in doing so they may overly reduce illuminance. This study proposed a method to optimize and compare the performance of different shading strategies by a multi-objective genetic algorithm (MOGA). An artificial neural network was combined into the optimization to efficiently reduce the simulation time. Meanwhile, based on data collected from a field survey, a formula was developed to calculate subjective satisfaction (daylight subjective vote, DSV) from the illuminance level. Considering the temporal and spatial performance of the daylight environment, we set the objective function by using the spatial glare autonomy (sGA) and spatial daylight vote autonomy (sDVA) based on DGP and DSV, separately. The proposed method was then used in a case study in a university library in Shanghai, China, to optimize and compare the performance of four shading strategies, namely, perforated aluminum sheet (PAS), vertical slats (Vs), serrated windows facing north (Sw_N), and serrated windows facing south (Sw_S). The following conclusions and contributions were made in this study:

- 1) The developed DSV formula described a quadratic relationship between horizontal illuminance level and subjective satisfaction with the daylight environment. The highest satisfaction was found to occur at approximately 1000 lux, and the satisfaction level declined with an increase or decrease in illuminance.

- 2) Under the climate of Shanghai, PAS and Sw_S had relatively bad performance among the four strategies; Serrated windows with northern have a better performance than serrated windows with southern.
- 3) A good shading device should be able to turn direct sunlight into diffusive one. Compared with the original design without shading strategies, the near-optimal designs for PAS, Vs, Sw_N, and Sw_S greatly reduced the complementary sGA0.35/95%, by 9%, 22%, 8%, and 8%, respectively, while maintaining a similar level of satisfaction with the daylight environment.

Credit author statement

Shikang Wen - Original draft preparation; Investigation; Formal analysis.
 Xiao Hu - Investigation.
 Guanjun Hua - Software; Validation;
 Peng Xue - Methodology.
 Dayi Lai - Writing - Review & Editing; Methodology; Funding acquisition.

Declaration of competing interest

The authors declare that they have no known competing financial interests or personal relationships that could have appeared to influence the work reported in this paper.

Data availability

Data will be made available on request.

Acknowledgement

This work was supported by the National Natural Science Foundation of China (Grant No. 52008242).

References

- [1] L. Pérez-Lombard, J. Ortiz, C. Pout, A review on buildings energy consumption information, *Energy Build.* 40 (3) (2008) 394–398.
- [2] S.A. Read, M.J. Collins, S.J. Vincent, Light exposure and eye growth in childhood, *Investig. Ophthalmol. Vis. Sci.* 56 (11) (2015) 6779–6787.
- [3] W. Wang, F. Wang, D. Lai, Q. Chen, Evaluation of SARS-CoV-2 transmission and infection in airliner cabins, *Indoor Air* 32 (1) (2022), e12979.
- [4] E. Vine, E. Lee, R. Clear, D. DiBartolomeo, S. Selkowitz, Office worker response to an automated Venetian blind and electric lighting system: a pilot study, *Energy Build.* 28 (2) (1998) 205–218.
- [5] R. Küller, C. Lindsten, Health and behavior of children in classrooms with and without windows, *J. Environ. Psychol.* 12 (4) (1992) 305–317.
- [6] P. Xue, C.M. Mak, H.D. Cheung, The effects of daylighting and human behavior on luminous comfort in residential buildings: a questionnaire survey, *Build. Environ.* 81 (2014) 51–59.
- [7] W. O'Brien, K. Kapsis, A.K. Athienitis, Manually-operated window shade patterns in office buildings: a critical review, *Build. Environ.* 60 (2013) 319–338.
- [8] A. Beck, W. Körner, O. Gross, J. Fricke, Making better use of natural light with a light-redirecting double-glazing system, *Sol. Energy* 66 (3) (1999) 215–221.
- [9] A.K. Yener, A method of obtaining visual comfort using fixed shading devices in rooms, *Build. Environ.* 34 (3) (1998) 285–291.
- [10] S.L. Torres, Y. Sakamoto, Facade design optimization for daylight with a simple genetic algorithm, *Proc. Build. Simul. Citeseer* (2007) 1162–1167.
- [11] M. Manzan, Genetic optimization of external fixed shading devices, *Energy Build.* 72 (2014) 431–440.
- [12] S. Vera, D. Uribe, W. Bustamante, G. Molina, Optimization of a fixed exterior complex fenestration system considering visual comfort and energy performance criteria, *Build. Environ.* 113 (2017) 163–174.
- [13] B. Lartigue, B. Lasternas, V. Loftness, Multi-objective optimization of building envelope for energy consumption and daylight, *Indoor Built Environ.* 23 (1) (2013) 70–80.
- [14] P. Xue, Q. Li, J. Xie, M. Zhao, J. Liu, Optimization of window-to-wall ratio with sunshades in China low latitude region considering daylighting and energy saving requirements, *Appl. Energy* 233–234 (2019) 62–70.
- [15] J.M.L. Gagne, M. Andersen, Multi-Objective Façade Optimization for Daylighting Design Using a Genetic Algorithm, 2010.
- [16] J. González, F. Fiorito, Daylight design of office buildings: optimisation of external solar shadings by using combined simulation methods, *Buildings* 5 (2) (2015).
- [17] A. Kirimtak, O. Krejcar, B. Ekici, M. Fatih Tasgetiren, Multi-objective energy and daylight optimization of amorphous shading devices in buildings, *Sol. Energy* 185 (2019) 100–111.
- [18] Y. Zhai, Y. Wang, Y. Huang, X. Meng, A multi-objective optimization methodology for window design considering energy consumption, thermal environment and visual performance, *Renew. Energy* 134 (2019) 1190–1199.
- [19] Z. Jalali, E. Noorzai, S. Heidari, Design and optimization of form and facade of an office building using the genetic algorithm, *Sci. Technol. Built. Environ.* 26 (2) (2020) 128–140.
- [20] P. Bakmohammadi, E. Noorzai, Optimization of the design of the primary school classrooms in terms of energy and daylight performance considering occupants thermal and visual comfort, *Energy Rep.* 6 (2020) 1590–1607.
- [21] E. Naderi, B. Sajadi, M.A. Behabadi, E. Naderi, Multi-objective simulation-based optimization of controlled blind specifications to reduce energy consumption, and thermal and visual discomfort: case studies in Iran, *Build. Environ.* 169 (2020), 106570.
- [22] P. Pilechiha, M. Mahdavinejad, F. Pour Rahimian, P. Carnemolla, S. Seyedzadeh, Multi-objective optimisation framework for designing office windows: quality of view, daylight and energy efficiency, *Appl. Energy* 261 (2020), 114356.
- [23] A.A.S. Bahdad, S.F.S. Fadzil, H.O. Onubi, S.A. BenLasod, Sensitivity analysis linked to multi-objective optimization for adjustments of light-shelves design parameters in response to visual comfort and thermal energy performance, *J. Build. Eng.* 44 (2021), 102996.
- [24] M. Ishac, W. Nadim, Standardization of optimization methodology of daylighting and shading strategy: a case study of an architectural design studio-the German University in Cairo, Egypt, *J. Build. Perform. Simul.* 14 (1) (2021) 52–77.
- [25] R.P. Khidmat, H. Fukuda, Kustiani, B. Paramita, M. Qingsong, A. Hariyadi, Investigation into the daylight performance of expanded-metal shading through parametric design and multi-objective optimisation in Japan, *J. Build. Eng.* 51 (2022), 104241.
- [26] J. Wienold, F. Frontini, S. Herkel, S. Mende, Climate Based Simulation of Different Shading Device Systems for Comfort and Energy Demand, 12th Conference of International Building Performance Simulation Association, 2011, pp. 14–16.
- [27] J.K. Day, B. Futrell, R. Cox, S.N. Ruiz, A. Amirazar, A.H. Zarabi, M. Azarbayjani, Blinded by the light: occupant perceptions and visual comfort assessments of three dynamic daylight control systems and shading strategies, *Build. Environ.* 154 (2019) 107–121.

- [28] G.J. Ward, The RADIANCE lighting simulation and rendering system, in: Proceedings of the 21st Annual Conference on Computer Graphics and Interactive Techniques, 1994, pp. 459–472.
- [29] N.L. Jones, Fast climate-based glare analysis and spatial mapping, in: Proceedings of Building Simulation 2019, 16th Conference of IBPSA, 2019.
- [30] I. Lm, Approved Method: IES Spatial Daylight Autonomy (sDA) and Annual Sunlight Exposure (ASE), Illuminating Engineering Society, 2013. <https://store.ies.org/product/ies-spatial-daylight-autonomy-sda-and-annual-sunlight-exposure-ase/>.
- [31] C.F. Reinhart, J. Mardaljevic, Z. Rogers, Dynamic daylight performance metrics for sustainable building design, LEUKOS 3 (1) (2006) 7–31.
- [32] L. Zhu, B. Wang, Y. Sun, Multi-objective optimization for energy consumption, daylighting and thermal comfort performance of rural tourism buildings in north China, Build. Environ. 176 (2020), 106841.
- [33] S. Wang, Y.K. Yi, N. Liu, Multi-objective optimization (MOO) for high-rise residential buildings layout centered on daylight, visual, and outdoor thermal metrics in China, Build. Environ. 205 (2021), 108263.
- [34] E. Nault, P. Moonen, E. Rey, M. Andersen, Predictive models for assessing the passive solar and daylight potential of neighborhood designs: a comparative proof-of-concept study, Build. Environ. 116 (2017) 1–16.
- [35] J. Ngarambe, A. Irakoze, G.Y. Yun, G. Kim, Comparative performance of machine learning algorithms in the prediction of indoor daylight illuminances, Sustainability 12 (11) (2020).
- [36] M. Ayoub, A review on machine learning algorithms to predict daylighting inside buildings, Sol. Energy 202 (2020) 249–275.
- [37] Z. Luo, C. Sun, Q. Dong, J. Yu, An innovative shading controller for blinds in an open-plan office using machine learning, Build. Environ. 189 (2021), 107529.
- [38] L. Magnier, F. Haghhighat, Multiobjective optimization of building design using TRNSYS simulations, genetic algorithm, and Artificial Neural Network, Build. Environ. 45 (3) (2010) 739–746.
- [39] R. ViEnnet, C. Fonteix, I. Marc, Multicriteria optimization using a genetic algorithm for determining a Pareto set, Int. J. Syst. Sci. 27 (2) (1996) 255–260.
- [40] L. Jiguan, Multiple-objective problems: Pareto-optimal solutions by method of proper equality constraints, IEEE Trans. Automat. Control 21 (5) (1976) 641–650.
- [41] N. Srinivas, K. Deb, Multiobjective optimization using nondominated sorting in genetic algorithms, Evol. Comput. 2 (3) (1994) 221–248.
- [42] S. Carlucci, G. Cattarin, F. Causone, L. Pagliano, Multi-objective optimization of a nearly zero-energy building based on thermal and visual discomfort minimization using a non-dominated sorting genetic algorithm (NSGA-II), Energy Build. 104 (2015) 378–394.
- [43] M. Hamdy, A. Hasan, K. Siren, Impact of adaptive thermal comfort criteria on building energy use and cooling equipment size using a multi-objective optimization scheme, Energy Build. 43 (9) (2011) 2055–2067.
- [44] A. Nabil, J. Mardaljevic, Useful daylight illuminance: a new paradigm for assessing daylight in buildings, Light. Res. Technol. 37 (1) (2005) 41–57.
- [45] A. Handina, N. Mukarromah, R.A. Mangkuto, R.T. Atmodipoero, Prediction of daylight availability in a large Hall with multiple facades using computer simulation and subjective perception, Procedia Eng. 170 (2017) 313–319.
- [46] S. Hu, M. He, G. Liu, M. Lu, P. Liang, F. Liu, Correlation between the visual evoked potential and subjective perception at different illumination levels based on entropy analysis, Build. Environ. 194 (2021), 107715.
- [47] Y. Bian, T. Luo, Investigation of visual comfort metrics from subjective responses in China: a study in offices with daylight, Build. Environ. 123 (2017) 661–671.
- [48] D.A. Chi, D. Moreno, J. Navarro, Design optimisation of perforated solar façades in order to balance daylighting with thermal performance, Build. Environ. 125 (2017) 383–400.
- [49] K.S. Lee, K.J. Han, J.W. Lee, The impact of shading type and azimuth orientation on the daylighting in a classroom—focusing on effectiveness of façade shading, comparing the results of DA and UDI, Energies 10 (5) (2017).
- [50] F.J. de Luis, M. Pérez-García, Parametric study of solar gains in saw-tooth roofs facing the equator, Renew. Energy 29 (8) (2004) 1223–1241.
- [51] M.R. Heras, M.J. Jiménez, M.J.S. Isidro, L.F. Zarzalejo, M. Pérez, Energetic analysis of a passive solar design, incorporated in a courtyard after refurbishment, using an innovative cover component based in a sawtooth roof concept, Sol. Energy 78 (1) (2005) 85–96.
- [52] I.R. Edmonds, P.J. Greenup, Daylighting in the tropics, Sol. Energy 73 (2) (2002) 111–121.
- [53] CIE, Lighting of Indoor Work Places, ISO 8995, 2002.
- [54] R.G. Hopkinson, Glare from daylighting in buildings, Appl. Ergon. 3 (4) (1972) 206–215.
- [55] H. Yang, B. Guo, Y. Shi, C. Jia, X. Li, F. Liu, Interior daylight environment of an elderly nursing home in Beijing, Build. Environ. 200 (2021), 107915.
- [56] K. Van Den Wymelenberg, M. Inanici, A critical investigation of common lighting design metrics for predicting human visual comfort in offices with daylight, LEUKOS 10 (3) (2014) 145–164.